Research
Microwave Wireless Power Transfer Technology—Article

# On Differentiation Among Pilot Signals of Multiple Mobile Targets in Retro-Reflective Beamforming for Wireless Power Transmission

Xin Wang [a], Long Li [b], Tie Jun Cui [c], Mingyu Lu [d],*

[a] School of Electrical Engineering, Chongqing University, Chongqing 400044, China
[b] School of Electronic Engineering, Xidian University, Xi'an 710071, China
[c] State Key Laboratory of Millimeter Waves, School of Information Science and Engineering, Southeast University, Nanjing 210096, China
[d] Department of Electrical and Computer Engineering, West Virginia University Institute of Technology, Beckley, WV 25801, USA

A R T I C L E   I N F O

A B S T R A C T

An experimental study is conducted on several retro-reflective beamforming schemes for wireless power transmission to multiple wireless power receivers (referred to herein as "targets"). The experimental results demonstrate that, when multiple targets broadcast continuous-wave pilot signals at respective frequencies, a retro-reflective wireless power transmitter is capable of generating multiple wireless power beams aiming at the respective targets as long as the multiple pilot signals are explicitly separated from one another by the wireless power transmitter. However, various practical complications are identified when the pilot signals of multiple targets are not appropriately differentiated from each other by the wireless power transmitter. Specifically, when multiple pilot signals are considered to be carried by the same frequency, the wireless power transmission performance becomes heavily dependent on the interaction among the pilot signals, which is highly undesirable in practice. In conclusion, it is essential for a retro-reflective wireless power transmitter to explicitly discriminate multiple targets' pilot signals among each other.

## 1. Introduction

With the rapid development of the Internet of Things, a vast number of small, low-cost, and low-power mobile electronic devices—such as radio-frequency identification tags and wireless sensors—will become integral parts of the society in the near future. Supplying electrical power to these devices wirelessly would eliminate or relieve their battery life limitation, and is therefore envisioned to be one of the enabling technologies for the next-generation Internet of Things [1,2]. The retro-reflective beamforming technique has excellent potential for accomplishing efficient wireless power transmission in the context of Internet of Things [3–7]. The fundamental scheme of retro-reflective beamforming includes two steps, as illustrated in Fig. 1. In the first step, pilot signals are broadcasted by one or more than one mobile devices as "request for wireless power," and the pilot signals detected by a wireless power transmitter are analyzed, as depicted

in Fig. 1(a). Based on the outcome of analyzing the pilot signals, the wireless power transmitter configures microwave power beam(s) toward the electronic device(s) in the second step, as shown in Fig. 1(b). As the primary merit of retro-reflective beamforming, the microwave power beams follow the devices' location dynamically, as long as the devices periodically broadcast pilot signals [8–12].

Although some numerical results show that retro-reflective beamforming is capable of tracking multiple wireless power receivers (referred to herein as "targets") and generating wireless power beams accordingly [13], most research efforts on retro-reflective beamforming in the literature include only one target in their experimental demonstrations (e.g. Refs. [3,4,7]). Indeed, once a retro-reflective wireless power transmitter is demonstrated to be successful in generating one wireless power beam in reaction to one target's pilot signal, it would generate multiple wireless power beams in response to pilot signals from multiple targets straightforwardly. Nevertheless, a theoretical study in Ref. [14] reveals that various serious complications will emerge when the pilot signals of multiple targets are not differentiated from one another by the retro-reflective wireless power transmitter.

* Corresponding author.
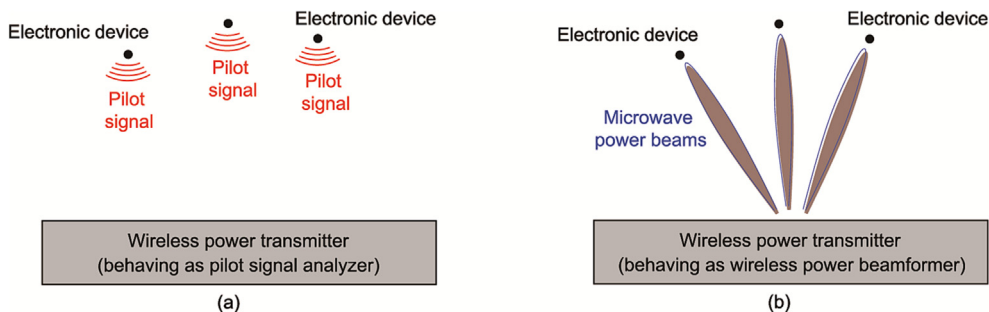  E-mail address: mingyu.lu@mail.wvu.edu (M. Lu).

**Fig. 1.** Illustration of the fundamental two-step scheme of retro-reflective beamforming for wireless power transmission to mobile electronic devices. (a) The first step: pilot signals are broadcasted by devices; (b) the second step: wireless power beams are generated toward the devices.

Inspired by the theoretical study of Ref. [14], an experimental system of digital retro-reflective beamforming is constructed in this paper. The wireless power transmitter includes an array of four antenna elements with a resonant frequency at 5.75 GHz. Multiple targets (i.e., multiple wireless power receivers) request the wireless power transmitter for power by broadcasting continuous-wave (CW) pilot signals at respective frequencies around 5.75 GHz. As long as the wireless power transmitter is able to explicitly resolve the pilot signals' frequencies, the wireless power transmitter is demonstrated to be capable of generating multiple wireless power beams aiming at the targets respectively. When two targets' pilot signals are considered to be located at the same frequency by the wireless power transmitter, however, the wireless power transmission performance becomes heavily dependent on the interaction between the two targets, which is highly undesirable in practice. It is therefore concluded that differentiating multiple targets' pilot signals from each other (via frequency division, time division, or code division) is necessary for a retro-reflective beamforming scheme to offer the optimal performance.

This paper is organized as follows. The experimental system of digital retro-reflective beamforming is described in Section 2. In Section 3, experimental results are presented to demonstrate the necessity of differentiating the pilot signals of multiple targets from each other. Finally, Section 4 summarizes our conclusions.

## 2. Experimental system of digital retro-reflective beamforming

The experimental system constructed in this research is portrayed in Fig. 2. The wireless power transmitter includes an array of four antenna elements deployed along the $x$ direction. The geo-metrical center of the four-element array is at ($x = 0$, $y = -1$ m, $z = 0$). One or more than one targets are located along the $x$ axis.

Microstrip antenna elements are employed in our experimental system. The front view of the four-element array in the wireless power transmitter is shown in Fig. 3. The microstrip patches are printed over a printed circuit board manufactured by Rogers Corporation (USA) with the model number RO4003C, a dielectric constant of 3.55, a thickness of 0.813 mm, and a loss tangent of 0.0027. Each antenna element is composed of four microstrip patches. Each microstrip patch has the physical dimensions of 13.4 mm × 13.4 mm, with a resonant frequency at 5.75 GHz. The wavelength in free space corresponding to the frequency 5.75 GHz, $\lambda_0$, is 52 mm. The distance between two adjacent antenna elements is about $0.77\lambda_0$. The feeding network (made of microstrip transmission lines) for the four microstrip patches in each element, which is visible in Fig. 3, is designed to ensure that the four patches are excited with an identical phase when the antenna element is used as a transmitting antenna. Each target includes only one antenna element that is identical to one of the antenna elements in Fig. 3.

The aperture of the antenna array in Fig. 3 has the physical dimensions $D \times D$, where $D$ is approximately 150 mm. According to the well-established far-field criterion in antenna engineering [15], a wireless power transmitter and a wireless power receiver reside in each other's far zone if the distance between them is greater than $2D^2/\lambda_0 = 0.86$ m. In the experimental setup shown
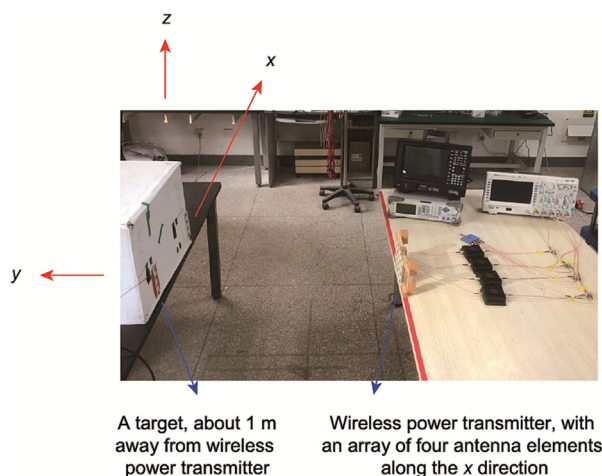


A target, about 1 m away from wireless power transmitter

Wireless power transmitter, with an array of four antenna elements along the $x$ direction

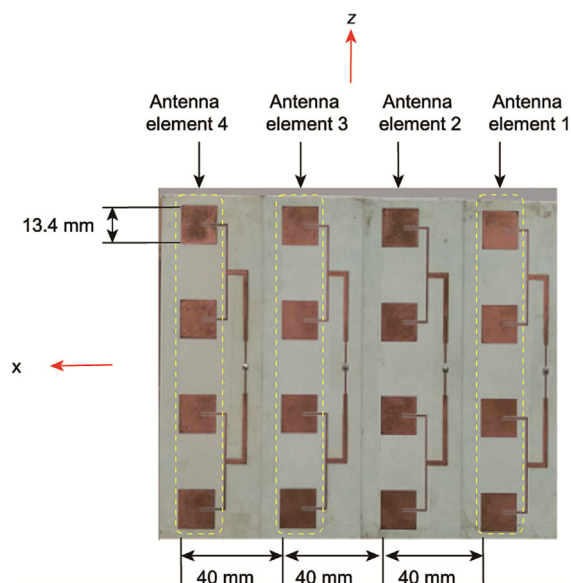**Fig. 2.** Photo of the experimental setup.



**Fig. 3.** Front view of the four-element antenna array in the wireless power transmitter.

in Fig. 2, the wireless power receiver is roughly 1 m away from the wireless power transmitter, barely satisfying the far-field condition. Since 1 m is not a large distance, a Cartesian coordinate system (rather than a spherical coordinate system) is adopted in this paper for presenting the experimental results.

The experimental characterization of one antenna element is presented in Fig. 4. One transmitting antenna element is located at ($x = 0, y = -1$ m, $z = 0$); it is connected to a CW power source with a frequency of 5.75 GHz and the transmitted power is $P_t$. One receiving antenna element moves along the $x$ axis; it is connected to a power meter, and the power measured by the power meter is denoted as the received power $P_r$. The power transmission efficiency $\eta$ is defined as $P_r/P_t$. According to the Friis transmission equation [15], $\eta$ can be formulated as follows:

$$\eta = \frac{P_r}{P_t} = (G_0)^2 \left(\frac{\lambda_0}{4\pi d}\right)^2 \tag{1}$$

where $d$ is the distance between the two antenna elements and $G_0$ is the gain value of one antenna element. The $G_0$ data obtained from Eq. (1) are plotted in Fig. 4 with respect to the $x$ coordinate of the receiving antenna element. It is observed from Fig. 4 that one antenna element has a fairly wide radiation beam along the $y$ direction. Each patch's gain along the broadside direction (i.e., the $y$ direction) is approximately 5 dB. Because the four patches included in one antenna element are excited with the same phase, the antenna element's gain at $x = 0$ is about 11 dB. Such a high gain associated with one antenna element lowers the requirements for the output power of the power amplifiers in the wireless power
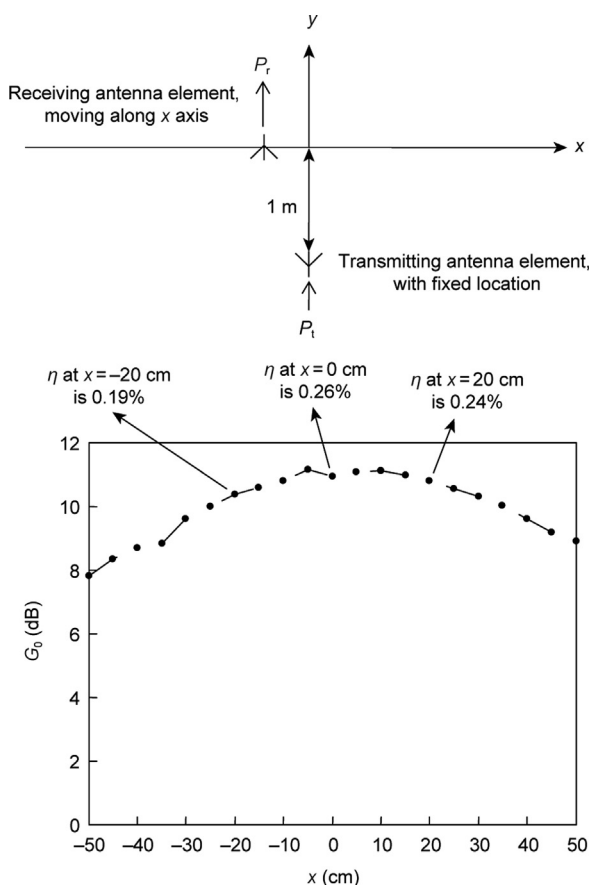


**Fig. 4.** $G_0$, the gain of one antenna element with respect to the $x$ coordinate of the receiving antenna element. $P_t$: the transmitted power; $P_r$: the received power; $\eta$: the power transmission efficiency.

transmitter, which in turn drastically alleviates the cost of our experiments.

The experiments on retro-reflective beamforming follow the two-step procedure shown in Fig. 1. In the first step, one or more than one targets broadcast pilot signals, and the wireless power transmitter analyzes the pilot signals. In the second step, the wireless power transmitter generates power beams toward the targets based on the outcome of analyzing the pilot signals.

The wireless power transmitter is constructed as a "digital retro-reflective beamformer." The pilot signals detected by the four antenna elements in the first step are amplified by four low-noise amplifiers respectively, down-converted to the intermediate-frequency band with the aid of four mixers, and then converted to the digital format using analog-to-digital converters. The four low-noise amplifiers are manufactured by Analog Devices (USA) with the model number ADL5611. The four mixers are purchased from Mini-Circuits (USA) with the model number SIM-73L+. A digital oscilloscope manufactured by Teledyne LeCroy (USA) with four channels is employed as the analog-to-digital converters. The pilot signals' information, including their frequency, amplitude, and phase, is obtained by processing the outputs of analog-to-digital converters. In the second step (i.e., the wireless power transmission step), the waveforms fed to the four antenna elements, which consist of one or multiple CW tones, are generated by a digital signal processing unit, converted to the analog format using digital-to-analog converters, up-converted to the 5.75 GHz frequency band, and pass through four power amplifiers before reaching the four antenna elements. The four digital-to-analog converters are implemented by two RIGOL DG4202 arbitrary waveform generators (each with two output channels). The frequency up-conversion is accomplished by four mixers with image rejection composed of 90° hybrid couplers JSPQ-65 W+ (manufactured by Mini-Circuits) along with in-phase/quadrature (I/Q) mixers HMC8193 (manufactured by Analog Devices). The power amplifiers employed in this work are HS5805Z1 signal boosters with a maximum output power of 5 W.

## 3. Experimental results of a comparative study of several retro-reflective beamforming schemes

The results collected from the experimental system outlined in Section 2 are presented in four subsections below.
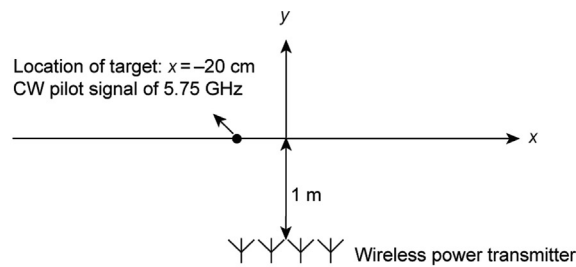
### 3.1. One target with a CW pilot signal of 5.75 GHz

The experimental setup of this subsection is illustrated at the top of Fig. 5. The experiment in this subsection includes two steps, as described next.

In the first step of retro-reflective beamforming, one target broadcasts a CW pilot signal of 5.75 GHz from location ($x = -20$ cm, $y = 0, z = 0$). The wireless power transmitter receives and analyzes the pilot signal. The pilot signals received by the four antenna elements of the wireless power transmitter are denoted in the time domain as $p_n(t) = A_n \cos(2\pi f t + \alpha_n)$, $n = 1, 2, 3, 4$, where $t$ is the variable standing for time, the frequency $f$ is 5.75 GHz, $\{A_1, A_2, A_3, A_4\}$ are the amplitude values of the four pilot signals, and $\{\alpha_1, \alpha_2, \alpha_3, \alpha_4\}$ are the phase values of the four pilot signals. With the aid of one local oscillator at 5.735 GHz, the pilot signals detected by the four antenna elements are down-converted to the intermediate frequency $f_{IF} = 15$ MHz. Four amplitudes $\{A_1, A_2, A_3, A_4\}$ and four phases $\{\alpha_1, \alpha_2, \alpha_3, \alpha_4\}$ are obtained at 15 MHz through Fourier transformation, as the outcome of the first step of retro-reflective beamforming. The normalized amplitude of $\{A_1, A_2, A_3, A_4\}$ (normalized by the largest value among $\{A_1, A_2, A_3, A_4\}$) and the phase values of $\{\alpha_1, \alpha_2, \alpha_3, \alpha_4\}$ are

displayed in two tables in Fig. 5. It is observed that the four amplitudes are quite uniform. It is also observed that $\alpha_2$, $\alpha_3$, and $\alpha_4$ decrease progressively with respect to $\alpha_1$, as expected.

In the second step of retro-reflective beamforming, a digital signal processing unit generates four waveforms $A_n \cos\{2\pi f_{IF}t - \alpha_n\}$, $n = 1, 2, 3, 4$. After these four waveforms are up-converted to 5.75 GHz using four mixers with image rejection, they are amplified and fed to the four antenna elements. Specifically, the four antenna elements are excited by $\gamma A_n \cos\{2\pi ft - \alpha_n\}$, $n = 1, 2, 3, 4$, where $\gamma$ is a real-valued constant. The profile of wireless power excitation in the second step of retro-reflective beamforming is the conjugate version of the pilot signal profile detected in the first step. The conjugate relationship between pilot signal reception and wireless power excitation ensures that the electromagnetic fields radiated by the four antenna elements are in phase at ($x = -20$ cm, $y = 0$, $z = 0$) in the second step of retro-reflective beamforming. The constant $\gamma$ represents the ratio between the amplitude of pilot signal reception and the amplitude of wireless power excitation. In practice, $\gamma$ is far greater than one and is determined by the power budget of the wireless power transmitter. A power meter is used to measure the power fed to each antenna element. The total amount of power fed to the four antenna elements is denoted as $P_t$. The target terminated by a power meter moves along the $x$ axis as the power detector. The power detected by the power meter is denoted as $P_r$.
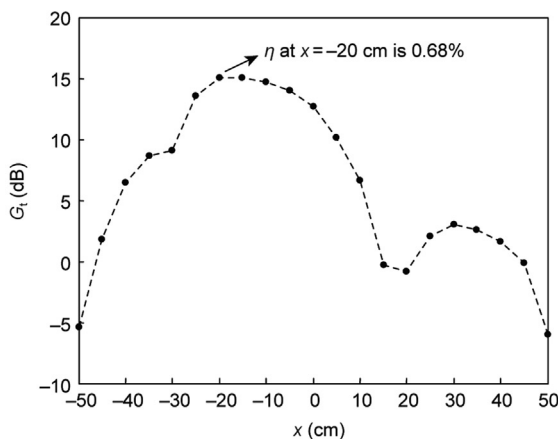
Some experimental results are plotted in Fig. 5, where the horizontal axis is the $x$ coordinate of the power detector and the vertical axis is $G_t$, the antenna gain of the four-element array. $G_t$ is calculated through the Friis transmission equation:

$$\eta = \frac{P_r}{P_t} = G_t G_0 \left(\frac{\lambda_0}{4\pi d}\right)^2 \tag{2}$$

When Eq. (2) is used to find $G_t$, $G_0$ is the gain value of one antenna element as shown in Fig. 4. One power beam is clearly visible in Fig. 5. The center of the power beam is at $x = -20$ cm, from which the pilot signal is broadcasted. The power transmission efficiency value at $x = -20$ cm is 0.68%, approximately four times greater than the efficiency value at $x = -20$ cm in Fig. 4. The fundamental scheme of retro-reflective beamforming aims to ensure that the radiations from the antenna elements of the wireless power transmitter are in phase at $x = -20$ cm. Since the excitation amplitudes to the four antenna elements in the second step of retro-reflective beamforming are almost uniform, the gain value at $x = -20$ cm would be enhanced by a factor of four [15], leading to a four-fold enhancement of the power transmission efficiency. Therefore, the experimental results in Fig. 5 agree with the fundamental theory of retro-reflective beamforming very well.

In the experiments of this subsection, one target requests wireless power via a CW pilot signal. In reaction to one CW pilot signal broadcasted by one target, the retro-reflective wireless power transmitter generates one power beam toward the target. This scenario has been investigated extensively in the literature (e.g., Refs. [3,4,7]). The results in this subsection serve as a benchmark for the subsequent subsections.

### 3.2. Two targets with respective CW pilot signals of 5.745 and 5.755 GHz

When multiple targets request wireless power simultaneously, they can be differentiated from one another by various possible means such as time division [16] and code division [17]. In this subsection, frequency division is applied to differentiate two targets from each other. The experimental setup of this subsection is illustrated at the top of Fig. 6. The experiment in this subsection includes two steps, as elaborated next.

In the first step, two targets, denoted as "target a" and "target b," broadcast pilot signals. Target a is located at ($x = -20$ cm, $y = 0$, $z = 0$), and its CW pilot signal is at the frequency of 5.745 GHz ($f^{(a)} = 5.745$ GHz). Target b is located at ($x = 20$ cm, $y = 0$, $z = 0$), and its CW pilot signal is at the frequency of 5.755 GHz ($f^{(b)} = 5.755$ GHz). The two pilot signals are individually generated by two oscillators that have similar output power levels. The pilot signals are received and analyzed by the wireless power transmitter. To be specific, the pilot signals received by the four antenna elements of wireless power transmitter are

$$p_n(t) = A_n^{(a)} \cos\left\{2\pi f^{(a)}t + \alpha_n^{(a)}\right\} + A_n^{(b)} \cos\left\{2\pi f^{(b)}t + \alpha_n^{(b)}\right\},$$
$$n = 1, 2, 3, 4 \tag{3}$$

With the aid of one local oscillator at 5.735 GHz, two intermediate frequency components at $f_{IF}^{(a)} = 10$ MHz and $f_{IF}^{(b)} = 20$ MHz are outstanding after down-conversion. $A_n^{(a)}$, $\alpha_n^{(a)}$, $A_n^{(b)}$, $\alpha_n^{(b)}$, $n = 1, 2, 3, 4$ are obtained through Fourier transforming the intermediate frequency components. Unsurprisingly, $\{A_1^{(a)}, A_2^{(a)}, A_3^{(a)}, A_4^{(a)}\}$ are quite uniform, and $\{A_1^{(b)}, A_2^{(b)}, A_3^{(b)}, A_4^{(b)}\}$ are quite uniform as well.



| Normalized $A_1$ | Normalized $A_2$ | Normalized $A_3$ | Normalized $A_4$ |
|---|---|---|---|
| 1.00 | 0.85 | 0.80 | 0.79 |

| Phase angle $\alpha_1$ | Phase angle $\alpha_2$ | Phase angle $\alpha_3$ | Phase angle $\alpha_4$ |
|---|---|---|---|
| 0 | −58° | −119° | −172° |

**Fig. 5.** Experimental results with one target broadcasting a CW pilot signal of 5.75 GHz. $G_t$ is the gain of the four-element array in reaction to the pilot signal. $\{A_1, A_2, A_3, A_4\}$: the amplitude of the four pilot signals; $\{\alpha_1, \alpha_2, \alpha_3, \alpha_4\}$: the phase of the four pilot signals.

In the second step of retro-reflective beamforming, four waveforms are generated as $A_n^{(a)} \cos\left\{2\pi f_{IF}^{(a)} t - \alpha_n^{(a)}\right\} + A_n^{(b)} \cos\left\{2\pi f_{IF}^{(b)} t - \alpha_n^{(b)}\right\}$, $n = 1, 2, 3, 4$ by a digital signal processing unit. After these four waveforms are up-converted and amplified, the waveforms fed to the four antenna elements are

$$q_n(t) = \gamma^{(a)} A_n^{(a)} \cos\left\{2\pi f^{(a)} t - \alpha_n^{(a)}\right\} + \gamma^{(b)} A_n^{(b)} \cos\left\{2\pi f^{(b)} t - \alpha_n^{(b)}\right\},$$
$$n = 1, 2, 3, 4 \tag{4}$$

In this subsection, $\gamma^{(a)} = \gamma^{(b)}$; in practice, however, the power budgets allocated to the two targets can be adjusted via $\gamma^{(a)}$ and $\gamma^{(b)}$. The time-average excitation power at the $n$th antenna element is $\left(\gamma^{(a)} A_n^{(a)}\right)^2/2 + \left(\gamma^{(b)} A_n^{(b)}\right)^2/2$, which is uniform among the four antenna elements. The transmitted power $P_t$ is measured by the same procedure as described in the previous subsection. One target terminated by a spectrum analyzer moves along the $x$ axis as the power detector. Here, a spectrum analyzer is used instead of a power meter such that the power values at $f^{(a)}$ and $f^{(b)}$ can be measured separately. The power measured at $f^{(a)}$ is denoted as $P_r^{(a)}$ and the power measured at $f^{(b)}$ is denoted as $P_r^{(b)}$.

Two curves are plotted in Fig. 6. The vertical axis associated with the blue curve is $G_t^{(a)}$, which is calculated using Eq. (2) with $P_r$ replaced by $P_r^{(a)}$. The vertical axis associated with the red curve in Fig. 6 is $G_t^{(b)}$, which is calculated using Eq. (2) with $P_r$ replaced by $P_r^{(b)}$. The wavelength $\lambda_0$ corresponding to 5.75 GHz is used in this subsection, as $f^{(a)}$ and $f^{(b)}$ are both very close to 5.75 GHz. The

horizontal axis of Fig. 6 is the $x$ coordinate of the power detector. Obviously, two power beams are generated by the wireless power transmitter. The power transmission efficiency values at $x = -20$ cm and $x = 20$ cm in Fig. 6 are approximately twice as much as those in Fig. 4, approaching the optimal performance of a four-element antenna array whose elements are excited with a uniform power.

In this subsection, the two power beams are independent of each other once the pilot signals of two targets are explicitly differentiated from each other by the wireless power transmitter. In other words, the power beam toward target a is completely dictated by the pilot signal from target a, and does not rely on the pilot signal from target b. It is possible that the wireless power transmitter may fail to differentiate the two pilot signals from each other in practice, especially when the two pilot signals' frequencies are close to each other, which is the scenario studied in the next subsection.

### 3.3. Two targets with CW pilot signals at the same frequency of 5.75 GHz

The physical configuration of this subsection is illustrated at the top of Figs. 7 and 8. Unlike the previous subsection, the two targets broadcast CW pilot signals at the same frequency of 5.75 GHz in this subsection. In our implementation, a CW signal at 5.75 GHz is generated by one oscillator and is then divided into two signals using a 1:2 power divider. The two output signals of the power divider are supplied to the two targets' antennas as the excitation of pilot signals, respectively. A phase shifter is applied before one of the two excitation signals reaches target b's antenna.
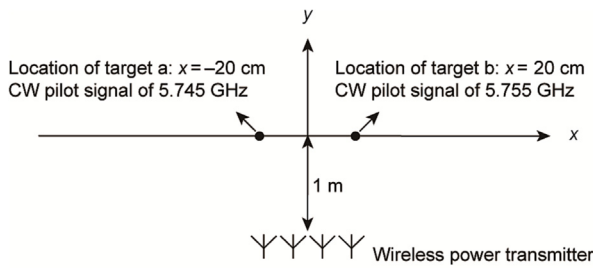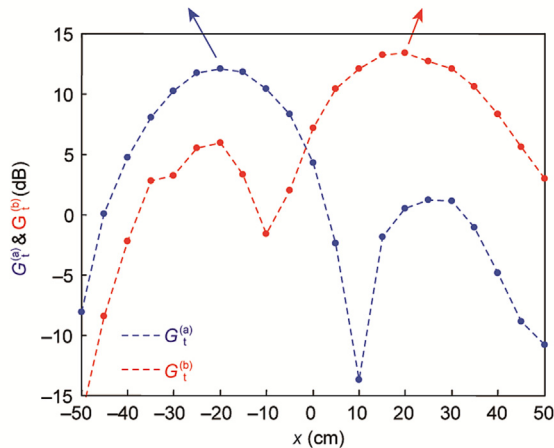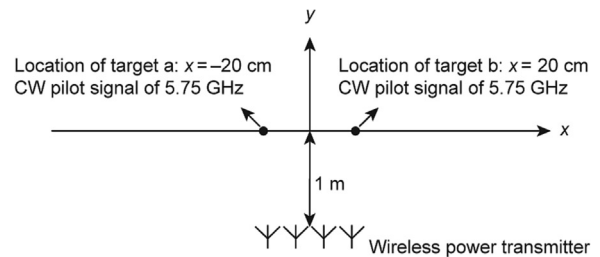


**Fig. 6.** Experimental results with two targets broadcasting CW pilot signals of 5.745 and 5.755 GHz respectively. $G_t^{(a)}$: the antenna gain of the four-element array at frequency $f^{(a)} = 5.745$ GHz; $G_t^{(b)}$: the antenna gain of the four-element array at frequency $f^{(b)} = 5.755$ GHz.



| Normalized $A_1$ | Normalized $A_2$ | Normalized $A_3$ | Normalized $A_4$ |
|---|---|---|---|
| 0.14 | 1.00 | 0.96 | 0.34 |

**Fig. 7.** Experimental results with two targets broadcasting CW pilot signals of the same frequency at 5.75 GHz. The phase difference between the excitations of two pilot signals is about 0.
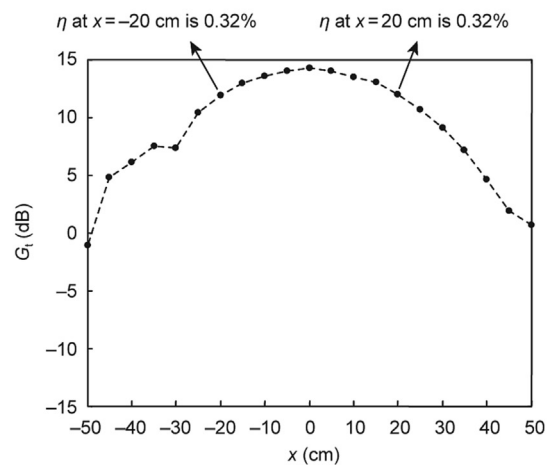
**Fig. 8.** Experimental results with two targets broadcasting CW pilot signals of the same frequency at 5.75 GHz. The phase difference between the excitations of two pilot signals is about 120°.
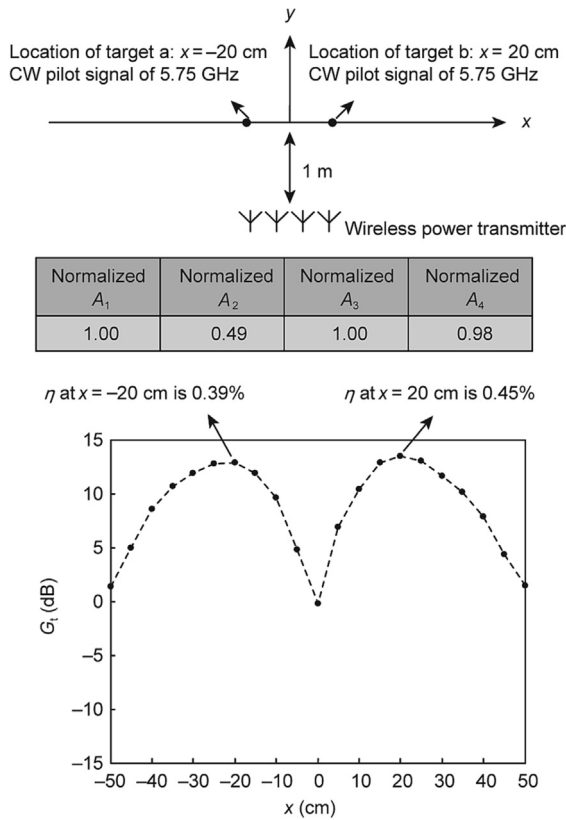
Consequently, the two excitation signals share the same frequency of 5.75 GHz, but the phase difference between them is tunable.

A total of 18 sets of experiments are carried out, as the phase delay created by the phase shifter is adjusted from 0 to 360° with 20° as the step size. Each set of experiments follows the procedure laid out in Section 3.1. Significant variations in the beamforming performance are observed among the 18 sets of experimental data, which indicate that the phase difference between the two pilot signals has a strong impact on the performance of the retro-reflective beamforming. Out of the 18 sets, two sets' results are presented in Figs. 7 and 8 to demonstrate the variations in the beamforming performance. The phase difference between the excitations of two pilot signals is about 0 in Fig. 7 and about 120° in Fig. 8.

In the first step of retro-reflective beamforming, the pilot signals detected by the four antenna elements of the wireless power transmitter are denoted as $p_n(t) = A_n \cos(2\pi ft + \alpha_n)$, $n$ = 1, 2, 3, 4, with $f$ = 5.75 GHz, as in Section 3.1. The interaction between the pilot signals from the two targets creates an interference pattern over the aperture of the four-element antenna array of the wireless power transmitter. Consequently, the four amplitude values $\{A_1, A_2, A_3, A_4\}$ are not uniform. In each of Figs. 7 and 8, the normalized values of $\{A_1, A_2, A_3, A_4\}$ (normalized by the largest value among $\{A_1, A_2, A_3, A_4\}$) are displayed in a table. In Fig. 7, when the pilot signals from the two targets reach the location of antenna element 1 or the location of antenna element 4, their phase difference is quite close to 180°; as a result, the sum of the two pilot signals has a weak amplitude. A different interference pattern is observed in Fig. 8: When the pilot signals from the two targets reach the location of antenna element 2, they significantly cancel each other.

In the second step of retro-reflective beamforming, the four antenna elements of the wireless power transmitter are excited by $\gamma A_n \cos\{2\pi ft - \alpha_n\}$, $n$ = 1, 2, 3, 4. The antenna gain of the four-element array, $G_t$, obtained from the measurement data is plotted in Figs. 7 and 8.

In Fig. 7, little wireless power is radiated by antenna element 1 or antenna element 4 in the second step of retro-reflective beamforming, since $A_1$ and $A_4$ are much smaller than $A_2$ and $A_3$. Thus, antenna elements 2 and 3 play dominant roles in the second step of retro-reflective beamforming. The four-element array is therefore almost equivalent to a two-element array in the wireless power transmission step. Since the two-element array (composed of antenna elements 2 and 3) has a smaller physical aperture than the four-element array, the power transmission efficiency values at $x$ = −20 cm and $x$ = 20 cm in Fig. 7 are lower than those in Fig. 6. The wireless power transmitter actually attempts to generate two beams, one toward $x$ = −20 cm and one toward $x$ = 20 cm. However, because of their large beamwidth, the two beams merge into one, as shown in Fig. 7. In Fig. 8, the fact that antenna element 2 is located at a "dark spot" of the interference pattern does not change the aperture size of the four-element array. As a result, the $G_t$ values of the two power beams in Fig. 8 are even higher than those in Fig. 6.

A comparison between the experimental results in this subsection and those in the previous subsection reveals that it is essential to explicitly discriminate the pilot signals of multiple targets from each other; in the previous subsection, a frequency division scheme is used to differentiate the multiple pilot signals from each other. If two targets' pilot signals can be differentiated from each other in frequency, the wireless power transmitter prepares the wireless power transmission to the two targets independently, as shown in the previous subsection. To be more specific, two power beams are generated by the wireless power transmitter toward the two targets, respectively. The two power beams are independent of each other in terms of the spatial focusing performance and power transmission efficiency. Moreover, the excitation power values to the antenna elements in the power transmission step are uniform. If two targets' pilot signals are carried by the same frequency, in contrast, the performance of retro-reflective beamforming depends on the interaction between the two pilot signals, as demonstrated in this subsection. Two power beams are generated by the wireless power transmitter toward the two targets respectively, which seems similar to the previous subsection. Nevertheless, the spatial focusing performance associated with the two power beams heavily depends on the phase difference between the two pilot signals, which would create a range of practical complications as elaborated below.

- When two targets broadcast pilot signals at the same frequency and when they are at similar distances from the wireless power transmitter, their pilot signals may create a strong interference pattern over the wireless power transmitter's aperture. A variety of interference patterns may appear, depending on the interaction between the two pilot signals; two examples are demonstrated in Figs. 7 and 8. Various interference patterns further result in various non-uniform amplitude profiles of the excitation to the antenna elements in the wireless power transmission step. Compared with the uniform amplitude profile in the previous subsection, the non-uniform amplitude profile sometimes leads to a poorer spatial focusing performance and sometimes leads to a better spatial focusing performance. At $x$ = 20 cm, for example, the power transmission efficiency is 0.32% in Fig. 7 but becomes 0.45% in Fig. 8. Moreover, as visualized in Figs. 7 and 8, the normalized $A_2$ (i.e., the excitation amplitude to antenna element 2) is 1.00 in Fig. 7 but becomes 0.49 in Fig. 8. If the total

amount of power transmitted by the wireless power transmitter has a fixed value, the power transmitted by antenna element 2 changes drastically between Figs. 7 and 8 (the ratio is about 8.1 dB, to be specific). As a result, the circuits (e.g., the power amplifier) associated with antenna element 2 are required to accommodate a wide dynamic range in terms of power level. In Fig. 6, in contrast, when the targets are differentiated from each other in frequency, the total amount of transmitted power is always uniformly dispatched among the antenna elements. Although exciting the antenna elements with a uniform power does not ensure the optimal performance of beamforming, a variety of practical complications would be avoided and the system complexity would be lowered.

- When two targets broadcast pilot signals at the same frequency while one target is farther away from the wireless power transmitter than the other target, the pilot signal from the farther target may be much weaker than that from the closer target. Consequently, the targets' pilot signals do not create a strong interference pattern over the aperture of wireless power transmitter. However, the wireless power transmitter will generate a strong power beam toward the closer target in reaction to its strong pilot signal and a weak power beam toward the farther target in reaction to its weak pilot signal. Such a power dispatching plan appears to be far from optimal. When the two pilot signals are told apart from each other in frequency (as demonstrated in Section 3.2), the strength of the two wireless power beams can be adjusted via $\gamma^{(a)}$ and $\gamma^{(b)}$, which facilitates better power management plans for the two targets.
- Obviously, the issues identified above would become more complicated and more serious if there are more than two targets and if the targets' pilot signals could not be differentiated among each other by the wireless power transmitter.

### 3.4. Three targets with respective CW pilot signals of 5.745, 5.750, and 5.755 GHz

Based on the experimental setup shown in Fig. 6, another target is included in this subsection. As depicted at the top of Fig. 9, three targets broadcast CW pilot signals at three different frequencies respectively. The scheme described in Section 3.2 can be straightforwardly extended to this subsection. As long as the wireless power transmitter is able to explicitly resolve the pilot signals of the three targets, three power beams are generated by the wireless power transmitter in reaction to the three targets' pilot signals, as observed from the experimental results in Fig. 9. Each power beam in Fig. 9 is solely dependent on one target's pilot signal; in other words, the interaction among the three targets' pilot signals does not affect the performance of retro-reflective beamforming. Moreover, the total amount of transmitted power is always distributed uniformly among the four antenna elements, thereby preventing various complications in circuit implementation.

In Section 3.2, there are two targets, and their pilot signals' frequencies are separated by 10 MHz. In this subsection, the three targets' pilot signals are separated among one another by 5 MHz. In all the experiments of this section, the temporal data length of Fourier transformation is as short as 200 ns. The temporal window of 200 ns corresponds to a spectral resolution of 5 MHz, which is sufficient to resolve the three pilot signals' frequencies of this subsection. Obviously, if more than three targets are allocated within the 10 MHz bandwidth, the temporal length of the Fourier transformation must be larger in order to refine the spectral resolution, which will increase the complexity of digital signal processing. In practice, numerous other factors (e.g., the drift of pilot signals' frequencies) must also be taken into account. Thus, when many targets are
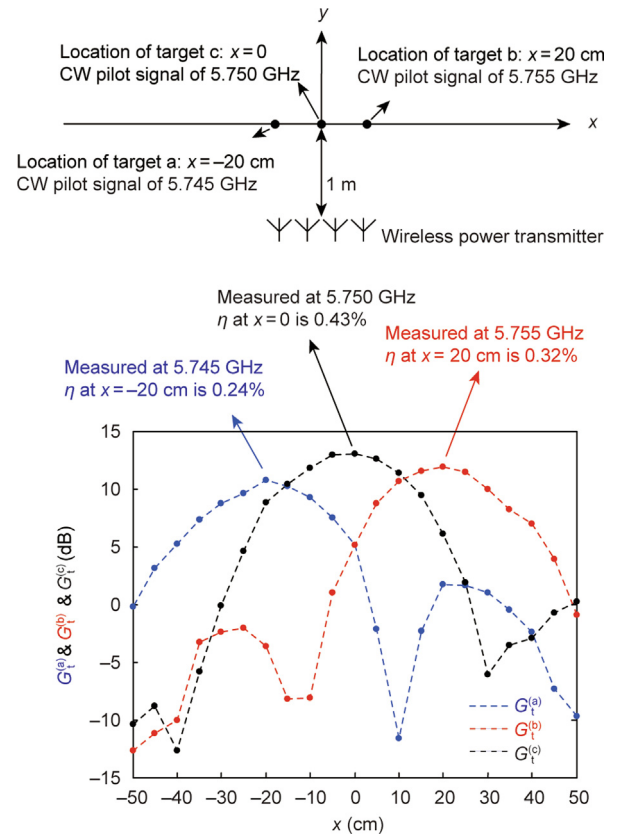


**Fig. 9.** Experimental results with three targets broadcasting CW pilot signals of 5.745, 5.750, and 5.755 GHz, respectively. $G_t^{(c)}$: the antenna gain of the four-element array at frequency $f^{(c)} = 5.75$ GHz.

densely populated within a certain frequency band, it is likely that the wireless power transmitter will fail to discriminate their pilot signals from each other. It should be noted that, if the wireless power transmitter fails to discriminate multiple pilot signals from each other, all the complications identified in Section 3.3 will ensue. Therefore, it does not appear to be the optimal resolution to merely rely on discriminating multiple targets' pilot signals in frequency. We are currently investigating various schemes to differentiate multiple targets from each other robustly.

The several retro-reflective beamforming schemes studied in this section, in which multiple microwave power beams are generated toward multiple targets respectively, can be considered as an analogy of the space division multiple access technique in wireless communication [18]. In wireless communication, the multiple beams are desired to achieve the best diversity among multiple targets. The top concern of wireless power transmission applications, however, is the optimal power transmission efficiency rather than diversity. Whereas tremendous research efforts have been devoted to the multi-beam technique in the context of wireless communication (as reviewed in Ref. [18]), the multi-beam technique with the optimal power transmission efficiency as the goal is much less explored. The experimental results of this section indicate that, in association with space division, it is imperative for another multiple access method (e.g., frequency division, time division, or code division) to be enforced in order to achieve the optimal power transmission efficiency. Although the work reported in this paper is far from sufficient to reach a complete resolution, we believe that it initiates an interesting direction for our further research. The digital retro-reflective beamforming system developed in this paper is able to accommodate diverse waveforms, since both the analysis of pilot signals and the generation of wireless power waveforms are carried out by digital signal

processing. We are endeavoring to take advantage of the digital retro-reflective beamforming system to explore various research topics such as those proposed in Refs. [19–21].

## 4. Conclusions

An experimental study is conducted on several retro-reflective beamforming schemes for wireless power transmission to multiple targets. Various practical complications are identified from the experimental results when the pilot signals of multiple targets are not appropriately differentiated from each other. It is concluded that, when multiple wireless power beams are generated toward multiple targets respectively in retro-reflective beamforming, it is necessary for a certain multiple access technique (based on frequency division, time division, or code division) to be enforced among the targets' pilot signals.

## Acknowledgments

## Compliance with ethics guidelines

Xin Wang, Long Li, Tie Jun Cui, and Mingyu Lu declare that they have no conflict of interest or financial conflicts to disclose.

## References

[1] Eid A, Hester JGD, Tentzeris MM. 5G as a wireless power grid. Sci Rep 2021;11:636.
[2] Li L, Zhang X, Song C, Zhang W, Jia T, Huang Y. Compact dual-band, wide-angle, polarization-angle-independent rectifying metasurface for ambient energy harvesting and wireless power transfer. IEEE Trans Microw Theory Tech 2021;69(3):1518–28.
[3] Wang X, Sha S, He J, Guo L, Lu M. Wireless power delivery to low-power mobile devices based on retro-reflective beamforming. IEEE Antennas Wirel Propag Lett 2014;13:919–22.
[4] He J, Wang X, Guo L, Shen S, Lu M. A distributed retro-reflective beamformer for wireless power transmission. Microw Opt Technol Lett 2015;57(8):1873–6.
[5] Cho YS. Development of transmitter/receiver front-end module with automatic Tx/Rx switching scheme for retro-reflective beamforming. J Inf Commun Converg Eng 2019;17(3):221–6.
[6] Koo H, Bae J, Choi W, Oh H, Lim H, Lee J, et al. Retroreflective transceiver array using a novel calibration method based on optimum phase searching. IEEE Trans Ind Electron 2020;68(3):2510–20.
[7] Wang X, Ruan B, Lu M. Retro-directive beamforming versus retro-reflective beamforming with applications in wireless power transmission. Prog Electromagn Res 2016;157:79–91.
[8] Park HS, Hong SK. A performance predictor of beamforming versus time-reversal based far-field wireless power transfer from linear array. Sci Rep 2021;11:22743.
[9] Takahashi T, Sasaki T, Homma Y, Mihara S, Sasaki K, Nakamura S, et al. Phased array system for high efficiency and high accuracy microwave power transmission. In: Proceedings of IEEE International Symposium on Phased Array Systems and Technology; 2016 Oct 18–21; Waltham, MA, USA; 2016.
[10] Khang ST, Lee DJ, Hwang IJ, Yeo TD, Yu JW. Microwave power transfer with optimal number of rectenna arrays for midrange applications. IEEE Antennas Wirel Propag Lett 2018;17(1):155–9.
[11] Hilario Re PD, Podilchak SK, Rotenberg SA, Goussetis G, Lee J. Circularly polarized retrodirective antenna array for wireless power transmission. IEEE Trans Antennas Propag 2020;68(4):2743–52.
[12] Fairouz M, Saed MA. A complete system of wireless power transfer using a circularly polarized retrodirective array. J Electromagn Eng Sci 2020;20(2):139–44.
[13] Zhai H, Pan HK, Lu M. A practical wireless charging system based on ultra-wideband retro-reflective beamforming. In: Proceedings of IEEE International Antennas and Propagation Symposium; 2010 Jul 11–17; Toronto, ON, Canada; 2010.
[14] Liu M, Wang X, Zhang S, Lu M. Theoretical analysis of retro-reflective beamforming schemes for wireless power transmission to multiple mobile targets. In: Proceedings of IEEE Wireless Power Transfer Conference; 2021 Jun 1–4; San Diego, CA, USA; 2021.
[15] Balanis CA. Antenna theory: analysis and design. 3rd ed. Hoboken: Wiley-Interscience; 2005.
[16] Pabbisetty G, Murata K, Taniguchi K, Mitomo T, Mori H. Evaluation of space time beamforming algorithm to realize maintenance-free IoT sensors with wireless power transfer system in 5.7-GHz band. IEEE Trans Microw Theory Tech 2019;67(12):5228–34.
[17] Sarin A, Avestruz AT. Code division multiple access wireless power transfer for energy sharing in heterogenous robot swarms. IEEE Access 2020;8:132121–33.
[18] Hong W, Jiang ZH, Yu C, Zhou J, Chen P, Yu Z, et al. Multibeam antenna technologies for 5G wireless communications. IEEE Trans Antennas Propag 2017;65(12):6231–49.
[19] Ibrahim R, Voyer D, Breard A, Huillery J, Vollaire C, Allard B, et al. Experiments of time-reversed pulse waves for wireless power transmission in an indoor environment. IEEE Trans Microw Theory Tech 2016;64(7):2159–70.
[20] Ku ML, Han Y, Lai HQ, Chen Y, Liu KJR. Power waveforming: wireless power transfer beyond time reversal. IEEE Trans Signal Process 2016;64(22):5819–34.
[21] Li B, Liu S, Zhang HL, Hu BJ, Zhao D, Huang Y. Wireless power transfer based on microwaves and time reversal for indoor environments. IEEE Access 2019;7:114897–908.